5   **2D dipping dike magnetic data interpretation using a robust particle swarm optimization**

Khalid S. Essa[1], Mahmoud El-Hussein[1*]

[1] Geophysics Department, Faculty of Science, Cairo University, Giza, P.O. 12613, Egypt.

Correspondence to: Mahmoud Elhussein (mahmoudelnouishy@yahoo.com)

10

Abstract. A robust Particle Swarm Optimization (PSO) investigation for magnetic data by a 2D dipping dike has been presented. The interpretive model parameters are: the amplitude coefficient (K), the depth to the top of the dipping dike (z), exact origin of the dipping dike (x_0), and the width of dipping dike (w). The inversion procedure is actualized to gauge the parameters of a 2D dipping dike structures where it has been confirmed first on synthetic models without

15   and with different level of random noise. The results of the inversion demonstrate that the parameters derived from the inversion concur well with the true ones. The root mean square (RMS) is figured by the strategy which is considered as the misfit between the measured and computed anomalies. The technique has been warily and effectively applied to real data examples from China and UK with the presence of ore bodies. The present technique can be applicable for mineral exploration and ore bodies of dike-like structure embedded in the shallow and deeper

20   subsurface.

1 Introduction

These days, tremendous measure of potential field data, for example, magnetic, gravity and SP data are gathered for the environmental and geological applications, including mineral, ores, oil exploration and groundwater investigations

25   (Reford and Sumner, 1964; Eppelbaum and Khesin, 2012; Essa et al., 2008; Holden et al., 2008; Paoletti et al., 2013; Mehanee, 2014a, Mehanee, 2014b; Pei et al., 2014; Eppelbaum, 2015; Mehanee, 2015; Mehanee and Essa, 2015; Abo-Ezz and Essa, 2016; Essa and Elhussein, 2016a; Maineult, 2016). The intrigued data here are the magnetic data gathered over dikes which considered as the most well-known geologic features and mineral carriers (Abdelrahman and Essa, 2005; Abdelrahman and Essa, 2015; Essa and Elhussein, 2016b; Al-Garni, 2015).

30   The estimation of model parameters (z, α, K, w, and x_0) of a buried 2D dipping dike structure is an essential target in interpretation of magnetic data. Thus, many published methods have presented for interpreting magnetic data, for example, the graphical method (Peters, 1949; Koulomzine et al., 1970; Rao and Murthy, 1978), Curve matching techniques (Hutchison, 1958; McGrath and Hood, 1970; Dondurur and Pamukcu, 2003), Fourier transform method (Bhimasankaram et al., 1978), correlation factors and integration nomograms (Atchuta Rao and Ram Babu, 1981;

35   Kara et al., 1996; Kara, 1997), the midpoint method (Murty, 1985), Hilbert transform method (Mohan et al., 1982;

Ram Babu and Atchuta Rao, 1991), Euler deconvolution method (Reid et al., 1990), Gauss- Newton method (Won, 1981), complex gradient method (Atchuta Rao et al., 1981), relation diagrams (Ram Babu et al., 1982), the gradient methods (Rao et al., 1973; Abdelrahman et al., 2007; Essa and Elhussein, 2016b), damped least-square ridge regression (Johnson, 1969), Spectral analysis methods (Bhattacharya, 1971; Sengupta and Das, 1975; Cassano and

40   Rocca, 1975), modular neural network inversion (Al-Garni, 2015), an automated numerical method (Keating and Pilkington, 1990), a new semi-automatic technique (Cooper, 2012), a non-linear constrained inversion technique (Beiki and Pedersen, 2012). However, the drawbacks of these methods are that they are highly subjective where they can lead to substantial errors in parameter estimations, rely upon trial and error till achieve the best fit between the measured and computed anomaly, require initial starting models which are close enough to the true solution, depends

45   on the precision of separation of regional and residual magnetic anomalies from the measured magnetic anomaly, either the dip of the dike or inclination of magnetic field is assumed for the guarantee of a good overall performance.

In this study, PSO is utilized for the magnetic anomalies due to 2D dipping dike to calculate the interpretive model parameters (z, α, K, w, and x_0). Our new approach was tested on synthetic data without and with different level of Gaussian noise (5%, 10%, 15%, and 20%). Here, we apply the new calculation on magnetic data by utilizing two

50   field cases from China and United Kingdom. So as to show the benefits the proposed design algorithm, the outcomes obtained are compared against borehole drilling information.

2 The method

The magnetic anomaly by a 2D dipping dike structure is given by (Hood, 1964; McGrath and Hood, 1970):

55   $T(x_i, z, d, \alpha) =$

$$K \left[\sin \alpha \left(\tan^{-1} \left(\frac{x_i + d}{z} \right) - \tan^{-1} \left(\frac{x_i - d}{z} \right) \right) - \frac{\cos \alpha}{2} \ln \left(\frac{(x_i + d)^2 + z^2}{(x_i - d)^2 + z^2} \right) \right],$$

$$i = 1, 2, 3, 4, \dots \dots \dots \dots . N \qquad (1)$$

where z is the depth (m) to the top, d is the half-width (m), α (deg.) is the index angle and K (mA/m) is the amplitude coefficient.

60   Kennedy and Eberhart, (1995) created a PSO-algorithm. It depends on the reproduction of the obvious social conduct of birds, fishes and insects in nourishment searching. PSO-calculation effectively connected and applied in many disciplines, like model development (Cedeno and Agrafiotis, 2003), biomedical pictures (Wachowiak et al., 2004), electromagnetic optimizations (Boeringer and Werner, 2004), hydrological issues (Chau, 2008), and different geophysical application (Alvarez et al., 2006; Shaw and Srivastava, 2007). In this calculation the birds representing

65   the particles or models, every particle has an area vector which represent the parameters value and a speed vector. For instance, for a five dimensional optimization issue, every particle or individual will have an area in a five dimensional space which represent an answer (Eberhart and Shi, 2001). Every particle changes its position at every

70 progression of the operation of the calculation, this position is updated during the iteration process considering the best position came to the particle which is known as the T_{best} model and the best area acquired any particle in the group which is known as the J_{best} model, this update is described in equation 2 and 3 (Sweilam et al., 2007)

$$V_i^{k+1} = c_3 V_i^k + c_1 \text{rand}()\left(T_{best} - P_i^{k+1}\right) + c_2 \text{rand}()\left[\left(J_{best} - P_i^{k+1}\right)P_i^{k+1}\right] = P_i^k + V_i^{k+1}, \quad (2)$$

$$x_i^{k+1} = x_i^k + v_i^{k+1}. \qquad (3)$$

75 where v_i^k is the speed of the particle i at the kth iteration, P_i^k is the current position of the ith particle at the kth iteration, rand() is a random number between 0 and 1, c_1 and c_2 are positive constant numbers known as cognitive coefficient and social coefficient, respectively, which control the individual and the social conduct, they are normally taken as 2 (Sweilam et al., 2007) yet some late researches provide that choosing c_1 greater than c_2 but c1+c2 ≤ 4 may give better results (Parsopoulos and Vrahatis, 2002), c_3 is the inertial coefficient which control the speed of the particle, since the

80 large values may make the particles miss up the good solutions and the small values may result in not enough search space for investigation (Sweilam et al., 2007), its typically taken less than 1, x_i^k is the position of the particle i at the kth iteration.

The five controlled-model parameters (z, K, θ, x_o, and w) can be estimated by applying the PSO-algorithm on the following objective function (Santos, 2010)

85

$$Q = \frac{2 \sum_{i=1}^N |T_i^m - T_i^c|}{\sum_{i=1}^N |T_i^m - T_i^c| + \sum_{i=1}^N |T_i^m + T_i^c|}, \qquad (4)$$

where N is the number of reading points, T_i^m is the measured magnetic anomaly at the point x_i, T_i^c is the calculated magnetic anomaly at the point x_i.

90 The magnetic anomaly from equation 1 is calculated at each iterative step for each x_i using the PSO-algorithm, Figure 1 represents the work flow of the PSO-algorithm, the RMS between the observed and calculated data is computed from the following formula:

$$RMS = \sqrt{\frac{\sum_{i=1}^N [T(x_i) - T_c(x_i)]^2}{N}}, \qquad (5)$$

where $T(x_i)$ is the measured field and $T_c(x_i)$ is the computed field. This is considered as the misfit between the

95 observed and calculated anomalies.

100   **3 Results**

In this paper, noisy free and contaminated data with different level of random noise (5, 10, 15, 20%) are utilized to exhibit the execution and appropriateness of the proposed technique**.**

3.1 Noise free data

The PSO-technique was applied to synthetic magnetic anomaly by a dipping dike with the following parameters; $K =$

105   795.78 mA/m, $z = 8$ m, $\alpha = 40^{\circ}$, $d = 3$, $x_o = 0$ m, and profile length = 80 m. In this situation, there is no noise in the data, so we begin test our procedure utilizing 100 models. The best model was come after 700 iterations and the ranges of the parameters are appeared in Table 1. The inverted-parameters that controlled the body dimensions have a good correspondence with the theoretical values (Table 1) which the percentage errors in the inverted-model parameters equal zero.

110   **3.2 Contaminated synthetic data**

Noisy-data considered as a critical part in geophysics. With a specific end goal to investigate the conduct of noise corrupted data.

At the principal, we forced 5% of arbitrary Gaussian noise on the magnetic data of the dipping dike model (Figure 2). The inverted-parameters (K, z, α, and d) are given in Table 1. Table 1 demonstrates that the rate of error in the inverted-

115   model parameters are 10%, 1.25%, 1.725%, 16.67%, respectively, and the RMs error is 3.49 mA/m.

Besides, we imposed 10% of arbitrary Gaussian noise on the same synthetic anomaly (Figure 3). The inverted-parameters (K, z, α, and d) are given in Table 1. Table 1 shows that the percentage of error in the inverted-model parameters are 13%, 1.25%, 0.9%, 20%, respectively, and the RMs error is 7.32 mA/m.

Thirdly, we embed 15% of random Gaussian noise on a similar synthetic anomaly (Figure 4). The inverted-parameters

120   (K, z, α, and d) are given in Table 1. Table 1 shows that the rate of error in the inverted-model parameters are 16.5%, 0%, 1.35%, 23.33%, respectively, and the RMs error is 13.59 mA/m.

At last, we imposed 20% of random Gaussian noise on a similar synthetic anomaly (Figure 5). The inverted-parameters (K, z, α, and d) are given in Table 1. Table 1 shows that the percentage of error in the inverted-model parameters are 20%, 2.5%, 1.2%, 16.67%, respectively, and the RMs error is 15.68 mA/m.

125   From the above outcomes, the estimations of the inverted-model parameters (K, z, α, d and x_o) for the synthetic example without and with various level of noise are in good correspondence with the true-values.

130

4 Field examples

Keeping in mind the end goal to inspect the productivity and the legitimacy of the suggested method, we have connected our new calculation to two real field cases with expanding complexity of the geological models taken from
135   the published literature.

4.1 Magnetic anomaly of Magnetite Iron Deposit, China

Figure 6 demonstrates the measured magnetic anomaly profile M163-1 in the magnetite iron deposit, Western Gansu Province, China (Guo et al., 1998) of length 222.5 m and the sampling interval is 2.78 m. This magnetic field anomaly is interpreted by the proposed method. Table 2 shows the ranges and results of estimated parameters ($K = 8116.91$
140   mA/m, $z = 22.24$ m, $\alpha = 57.99°$, $d = 9.174$, $x_o = 0.01$ m). The evaluated model has been computed and contrasted with the true ones (Figure 6). The final outcomes computed are contrasted with the borehole drilling information ($z = 20$-25 m and $d = 9$ m) as far as various parameters (Table 3).

4.2 Magnetic anomaly in Red Hill Farm, UK

In this part, we will utilize a PSO algorithm to evaluate the interpretive model parameters of magnetic anomaly profile
145   taken in south of Red Hill Farm, Millom, United Kingdom (Hallimond and Whetton, 1939). The length of the profile is 61 m and the digitizing interval is 0.76 m (Figure 7). This magnetic field anomaly is interpreted by the proposed method. Table 4 demonstrates the ranges and outcomes of estimated parameters ($K = 175.07$ mA/m, $z = 19$ m, $\alpha = 75.6°$, $d = 2.28$ m, $x_o = -0.1$). The estimated model has been computed and contrasted with the true ones (Figure 7) There is a good correlation between results assessed from our technique and the borehole drilling information
150   published in Hallimond and Whetton (1939) (where $z = 18.29$ m and $d = 2.29$ m).

At last, we assess the adequacy and proficiency of our technique, we additionally contrast its execution with some state of art algorithms. Tables 2 and 4 condense the inverted results. As can be found in these tables, surprisingly, our inversion algorithm significantly outperforms the up-to-date model parameters estimation for two field examples. For all field example, our inversion gives a full picture of the model parameters rather than other methods which did not
155   give a fully interpretation.

160

5 Conclusions

This paper illustrated the utilization of new algorithm in assessing the model parameters (z, x_o, d, α and K) of a 2D

165   dipping dike model. The viability of the suggested algorithm is exhibited on five troublesome examples including noisy free data, contaminated data, and two real field data. The new approach has the ability to get the better quality solution, and has better convergence characteristics and computational efficiency. The comparison of the results with drilling information reported in the literature demonstrated the prevalence of the suggested method and its potential for solving magnetic problem. From the outcomes obtained, it is finished up new inversion algorithm is a promising

170   technique for solving the quantitative interpretation of magnetic data. In the future work, we will attempt to propose some enhanced version of this new inversion algorithm to solve the problem.

6 Data availability

First our algorithm is applied on synthetic data created from equation 1 with and without Gaussian noise (Hood,

175   1964; McGrath and Hood, 1970), the results were given in section 3. Then the proposed algorithm applied to two field examples the first one is profile over the magnetite iron deposit, Western Gansu Province, China (Guo et al., 1998) of length 222.5 m (Figure 6) and the sampling interval is 2.78 m, while the second one was magnetic anomaly profile taken in south of Red Hill Farm, Millom, United Kingdom (Hallimond and Whetton, 1939). The profile length is 61 m and the sampling interval is 0.76 m (Figure 7).

180

185

190

Geoscientific
Instrumentation
Methods and
Data Systems
Discussions

References

Abdelrahman, E. M., Abo-Ezz, E. R., Soliman, K. S., EL-Araby, T. M., and Essa, K. S.: A Least-squares Window Curves Method for Interpretation of Magnetic Anomalies Caused by Dipping Dikes, Pure Appl. Geophys., 164, 1027–1044, 2007.

Abdelrahman, E. M., EL-Araby, H. M., EL-Araby, T. M., and Essa, K. S.: A Least-squares Minimization Approach to Depth Determination from Magnetic Data, Pure Appl. Geophys., 160, 1259–1271, 2003.

Abdelrahman, E. M., and Essa, K. S.: Magnetic interpretation using a least-squares, depth-shape curves method, Geophysics, 70, L23-L30, 2005.

Abdelrahman, E. M., and Essa, K. S.: A new method for depth and shape determinations from magnetic data, Pure Appl. Geophys., 172, 439–460, 2015.

Abo-Ezz, E. R., and Essa, K. S.: A least-squares minimization approach for model parameters estimate by using a new magnetic anomaly formula, Pure Appl. Geophys., 173, 1265-1278, 2016.

Al-Garni, M. A.: Interpretation of magnetic anomalies due to dipping dikes using neural network inversion, Arab. J. Geosci., 8, 8721-8729, 2015.

Alvarez, J. P. F., Martìnez, F., Gonzalo, E. G., and Pèrez, C. O. M.: Application of the particle swarm optimization algorithm to the solution and appraisal of the vertical electrical sounding inverse problem, in: proceedings of the 11th Annual Conference of the international Association of Mathematical Geology (IAMG06), Li_ege, Belgium, CDROM, 2006.

Atchuta Rao, D., and Ram Babu, H. V.: Nomograms for Rapid Evaluation of Magnetic Anomalies over Long Tabular Bodies, Pure Appl. Geophys., 119, 1037–1050, 1981.

Atchuta Rao, D., Ram Babu, H. V., and Sanker Narayan, P. V.: Interpretation of magnetic anomalies due to dikes: The complex gradient method, Geophysics, 46, 1572-1578, 1981.

Beiki, M., and Pederson, L. B.: Estimating magnetic dike parameters using a non-linear constrained inversion technique: an example from the Särna area, west central Sweden, Geophys. Prospect., 60, 526-538, 2012.

Bhattacharya, B.: Analysis of a vertical dyke infinitely deep, striking north by Fourier transform, Pure Appl. Geophys., 89, 134-138, 1971.

Bhimasankaram, V. L. S., Mohan, N. I., and Seshagiri Rao, S. V.: Interpretation of magnetic anomalies of dikes using Fourier transforms, Geophysical exploration, 16, 259-266, 1978.

Boeringer, D. W., and Werner, D. H.: Particle swarm optimization versus genetic algorithms for phased array synthesis, IEEE Transactions on Antennas and Propagation 52, 771–779, 2004.

Bruckshaw, J. M., and Kunaratnam, K.: The Interpretation of magnetic anomalies due to dykes, Geophys. Prospect., 11, 509-522, 1963.

Cassano, E., and Rocca, F.: Interpretation of magnetic anomalies using spectral estimation techniques, Geophys. Prospect., 23, 663-681, 1975.

Cedeno, W., and Agrafiotis, D. K.: Using particle swarms for the development of QSAR models based on K-nearest neighbor and kernel regression, J COMPUT AID MOL DES., 17, 255–263, 2003.

Chau, W. K.: Application of a particle swarm optimization algorithm to hydrological problems, in L. N. Robinson (Ed.), Water Resources Research Progress: Nova Science Publishers Inc., New York, 3–12pp, 2008.

230   Cooper, G. R. J.: The semi-automatic interpretation of magnetic dyke anomalies, Comput. Geosci., 44, 95-99, 2012.

Dondurur, D., and Pamukçu, O.A.: Interpretation of magnetic anomalies from dipping dike model using inverse solution, power spectrum and Hilbert transform methods, J. Balk. Geo. Soc., 6, 127-139, 2003.

Eberhart, R. C., and Shi, Y.: Particle swarm optimization: developments, applications and resources, in Proceedings of the Congress on Evolutionary Computation, Seoul, Korea, 81–86, 2001.

235   Eppelbaum, L. V.: Quantitative interpretation of magnetic anomalies from bodies approximated by thick bed models in complex environments, Environ. Earth Sci., 74, 5971-5988, 2015.

Eppelbaum, L. V., and Khesin, B. E.:   Geophysical Studies in the Caucasus, Springer, 411p, 2012..

Essa, K. S., and Elhussein, M.: A new approach for the interpretation of magnetic data by a 2-D dipping dike, J. Appl. Geophys., doi: 10.1016/j.jappgeo.2016.11.022, 2016a.

240   Essa, K. S., and Elhussein, M.: A new approach for the interpretation of self-potential data by 2-D inclined plate, J. Appl. Geophys., doi: 10.1016/j.jappgeo.2016.11.019, 2016b.

Essa, K. S., Mehanee, S., and Smith, P. D.: A new inversion algorithm for estimating the best fitting parameters of some geometrically simple body to measured self-potential anomalies, Explor. Geophys., 39, 155–163, 2008.

Guo, W., Dentith, M. C., Li, Z., and Powell, C. M.: Self demagnetization corrections in magnetic modeling: some
245   examples, Explor. Geophys., 29, 396-401, 1998.

Hallimond, A. F., and Whetton, J. T.: Magnetic Survey of Hematite Ore In South Cumberland And Furness, Bulletin of the GEOLOGICAL SURVEY OF GREAT BRITAIN, 2, 1-17, 1939.

Holden, E. J., Dentith, M., and Kovesi, P.: Towards the automatic analysis of regional aeromagnetic data to identify regions prospective for gold deposits, Comput. Geosci., 34, 1505–1513, 2008.

250   Hood, P.: The Königsberger ratio and the dipping-dyke equation, Geophys. Prospect., 12, 440–456, 1964.

Hutchison, R. D.: Magnetic analysis by logarithmic curves, Geophysics, 23, 749-769, 1958.

Johnson, W. W.: A least squares method of interpreting magnetic anomalies caused by two dimensional structures, Geophysics, 34, 65–74, 1969.

Kara, I.: Magnetic interpretation of two-dimensional dikes using integration-nomograms, J. Appl. Geophys., 36, 175-
255   180, 1997.

Kara, I., Özdemir, M., and Yuksel, F. A.: Interpretation of magnetic anomalies of dikes using correlation factors, Pure Appl. Geophys., 147, 777–788, 1996.

Keating, P. B., Pilkington, M.: An automated method for the interpretation of magnetic vertical-gradient anomalies, Geophysics, 55, 336-343, 1990.

260   Kennedy, J., and Eberhart, R.: Particle Swarm Optimization, IEEE Intemational Conference on Neural Networks (Perth, Australia): IEEE Service Center, PiscatawaY, NJ, lV, 1942-1948, 1995.

Koulomzine, T., Lamontagne, Y., and Nadeau, A.: New methods for the direct interpretation of magnetic anomalies caused by inclined dikes of infinite length, Geophysics, 35, 812-830, 1970.

265   Maineult, A.: Estimation of the electrical potential distribution along metallic casing from surface self-potential
            profile, J. Appl. Geophys., 129, 66-78, 2016.

       Mcgrath, P. H., and Hood, P. J.: The dipping dike case, a computer curve matching method of magnetic interpretation,
            Geophysics, 35, 831-848, 1970.

       Mehanee, S.: Accurate and efficient regularized inversion approach for the interpretation of isolated gravity anomalies,
270   Pure Appl. Geophys., 171, 1897–1937, 2014a.

       Mehanee, S.: An efficient regularized inversion approach for self potential data interpretation of ore exploration using
            a mix of logarithmic and non-logarithmic model parameters, Ore Geol. Rev., 57, 87–115, 2014b.

       Mehanee, S.: Tracing of paleo-shear zones using self-potential data inversion: case studies from the KTB, Rittsteig,
            and Grossensees graphite-bearing fault planes, Earth Planets Space, 67, 14–47, 2015.

275   Mehanee, S. A., and Essa, K. S.: 2.5D regularized inversion for the interpretation of residual gravity data by a dipping
            thin sheet: numerical examples and case studies with an insight on sensitivity and non-uniqueness, Earth
            Planets Space, 67, 130, 1-26, 2015.

       Mohan, N. L., Sundararajan, N., and Seshagiri Rao S. V.: Interpretation of Some Two-Dimensional Magnetic Bodies
            Using Hilbert Transforms, Geophysics, 47, 376-387, 1982.

280   Murthy, I. V. R.: The midpoint method: Magnetic interpretation of dikes and faults, Geophysics, 50, 834-839, 1985.

       Paoletti, V., Ialongo, S., Florio, G., Fedi, M., and Cella, F.: Self-constrained inversion of potential fields, Geophysical
            Journal International, 195, 854–869, 2013.

       Parsopoulos, K. E., and Vrahatis, M. N.: Recent approaches to global optimization problems through Particle Swarm
            Optimization, Natural Computing, 1, 235-306, 2002.

285   Pei, J., Li, H., Wang, H., Si, J., Sun, Z., and Zhou, Z.: Magnetic properties of the Wenchuan Earthquake Fault Scientific
            Drilling Project Hole-1 (WFSD-1), Sichuan Province, China. Earth Planets Space, 66:23, 1-12, 2014, 2014.

       Petres, L. J.: Direct approach to magnetic interpretation and its practical application, Geophysics 14, 290-320, 1949.

       Ram Babu, H. V., and Atchuta Rao, D.: Application of the Hilbert Transform for Gravity and Magnetic Interpretation,
            Pure Appl. Geophys., 135, 589-599, 1991.

290   Ram Babu, H. V., Subrahmanyam, A. S., and Atchuta Rao, D.: A Comparative Study of the Relation Figures of
            Magnetic Anomalies due to Two-dimensional Dike and Vertical Step Models, Geophysics, 47, 926–931,
            1982.

       Rao, B. S. R., and Murthy, I. V. R.: Gravity and magnetic methods of prospecting. Arnold-Heinemann Publishers
            (India) Pvt. Ltd., New Delhi, 1978.

295   Rao, B. S. R., Murthy, I. V. R., and Rao, C. V.: Two methods for computer interpretation of magnetic anomalies of
            dikes, Geophysics, 38, 710–718, 1973.

       Reford, M. S., and Sumner, J. S.: Aeromagnetics, Geophysics, 29, 482–516, 1964.

       Reid, A. B., Allsop, J. M., Millett, A. J., and Somerton, I. W.: Magnetic interpretation in three dimensions using Euler
            deconvolution, Geophysics, 55, 80-91, 1990.

300   Santos, F. A. M.: Inversion of self – potential of idealized bodies’ anomalies using particle swarm optimization,
            Comput. Geosci., 36, 1185–1190, 2010.

Sengupta, S., Das, S. K.: Interpretation of magnetic anomalies of dikes by Fourier transforms, Pure Appl. Geophys., 113, 625-633, 1975.

Shaw, R. and Srivastava, S.: Particle swarm optimization: a new tool to invert geophysical data, Geophysics, 72, 75–83, 2007.

305

Sweilam, N. H., El-Metwally, K., and Abdelazeem, M.: Self potential signal inversion to simple polarized bodies using the particle swarm optimization method: A visibility study, J. Appl. Geophys., 6, 195-208, 2007.

Wachowiak, M. P., Smolı́kova´, R., Zheng, Y., Zurada, J. M., and Elmaghraby, A. S.: An approach to multimodal biomedical image registration utilizing particle swarm optimization, IEEE Transactions on Evolutionary

310

Computation, 8, 289–301, 2004.

Won, I. J.: Application of Gauss's method to magnetic anomalies of dipping dikes, Geophysics, 46, 211–215, 1981.

315

320

325

330

Table 1. Numerical results for a 2D dipping dike model without and with various level of 5%, 10%, 15%, and 20% of Gaussian noise (K = 795.78 mA/m, z = 7 m, α = 40 º, d = 3, x_o = 0 m, and profile length = 80 m).

Type of body	Parameters	Used ranges	Result	e (%)	RMS (mA/m)
Dipping dike	without random Gaussian noise				
	K (mA/m)	397.89-1591.55	795.78	0	
	z (m)	1-12	8	0	
	α (º)	10-60	40	0	0
	d (m)	1-8	3	0	
	x_o (m)	-80-30	0	0	
	with 5% random Gaussian noise				
	K (mA/m)	397.89-1591.55	875.35	10	
	z (m)	1-12	8.1	1.25	
	α (º)	10-60	39.31	1.725	3.49
	d (m)	1-8	2.5	16.67	
	x_o (m)	-80-30	0.11	------	
	with 10% random Gaussian noise				
	K (mA/m)	397.89-1591.55	899.23	13	
	z (m)	1-12	8.1	1.25	
	α (º)	10-60	40.36	0.9	7.32
	d (m)	1-8	2.4	20	
	x_o (m)	-80-30	-0.08	------	
	With 15% random Gaussian noise				
	K (mA/m)	397.89-1591.55	927.08	16.5	
	z (m)	1-12	8	0	
	α (º)	10-60	39.46	1.35	13.59
	d (m)	1-8	3.7	23.33	
	x_o (m)	-80-30	0.10	------	
	With 20% random Gaussian noise				
	K (mA/m)	397.89-1591.55	954.93	20	
	z (m)	1-12	7.8	2.5	
	α (º)	10-60	40.48	1.2	15.68
	d (m)	1-8	2.5	16.67	
	x_o (m)	-80-30	-0.25	------	

335

Geoscientific
Instrumentation
Methods and
Data Systems
Open Access
EGU
Discussions

Table 2. Numerical results for the magnetite iron deposit field example, China.

340

Parameters	Used Ranges	Result	RMS (mA/m)
K (mA/m)	79.58-1591.55	8116.91	
z (m)	16-28	22.24	
α (°)	20-80	57.99	198.73
d (m)	5-12	9.174	
x_o (m)	-10-10	0.01	

345 **Table 3. Correlation between numerical results obtained from drilling data and our method for magnetite iron deposit field example, China.**

Method / Parameters	Drilling data, Guo, et al. (1998)	Present method
K (mA/m)	-------	8116.91
z (m)	22-25	22.24
α (°)	-------	57.99
d (m)	9	9.174
x_o (m)	--------	0.01

350

Table 4. Numerical results for magnetic anomaly in Red Hill Farm, UK field example.

Parameters	Used Ranges	Result	RMS (mA/m)
K (mA/m)	79.58-795.78	175.07	
z (m)	20-30	19	
α (°)	20-90	75.6	0.74
d (m)	1-10	2.28	
x_o (m)	-10-10	0.1	

355

360

365

370

375

380

385

390

395

400
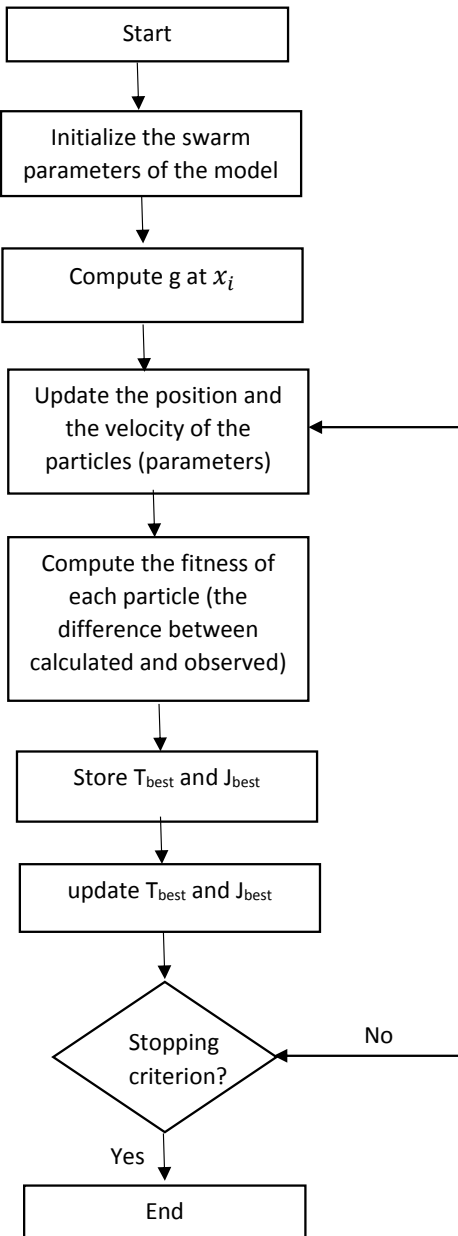
Figure 1: work-flow of PSO-algorithm applied to magnetic anomalies interpretation

405

Geoscientific
Instrumentation
Methods and
Data Systems
Discussions

Open Access

410

415

420

425
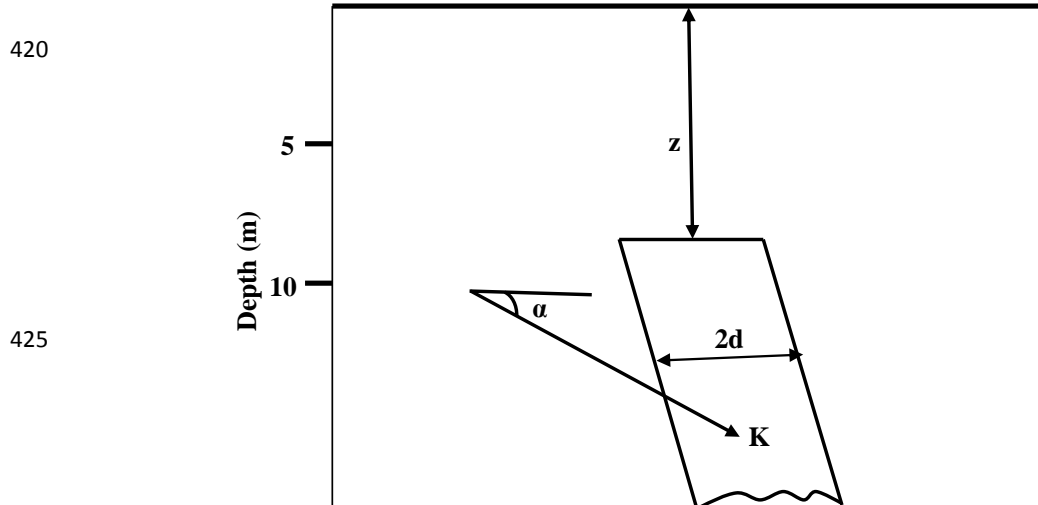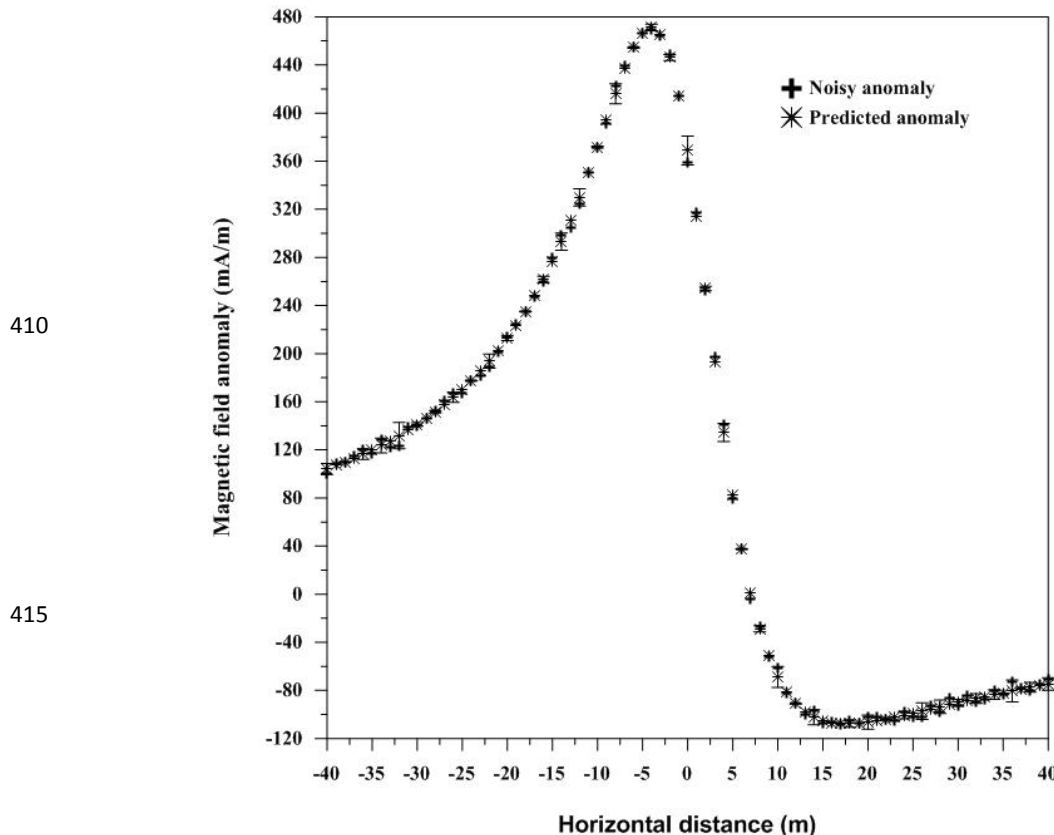
Figure 2: Total magnetic anomaly of a buried dipping dike-like a geologic structure with K = 795.78 mA/m, z

430   **= 8 m, α = 40º, d= 3, x_0 = 0 m, and profile length = 80 m, without and with 5% random Gaussian**

noise.

Geoscientific
Instrumentation
Methods and
Data Systems
Discussions

Open Access
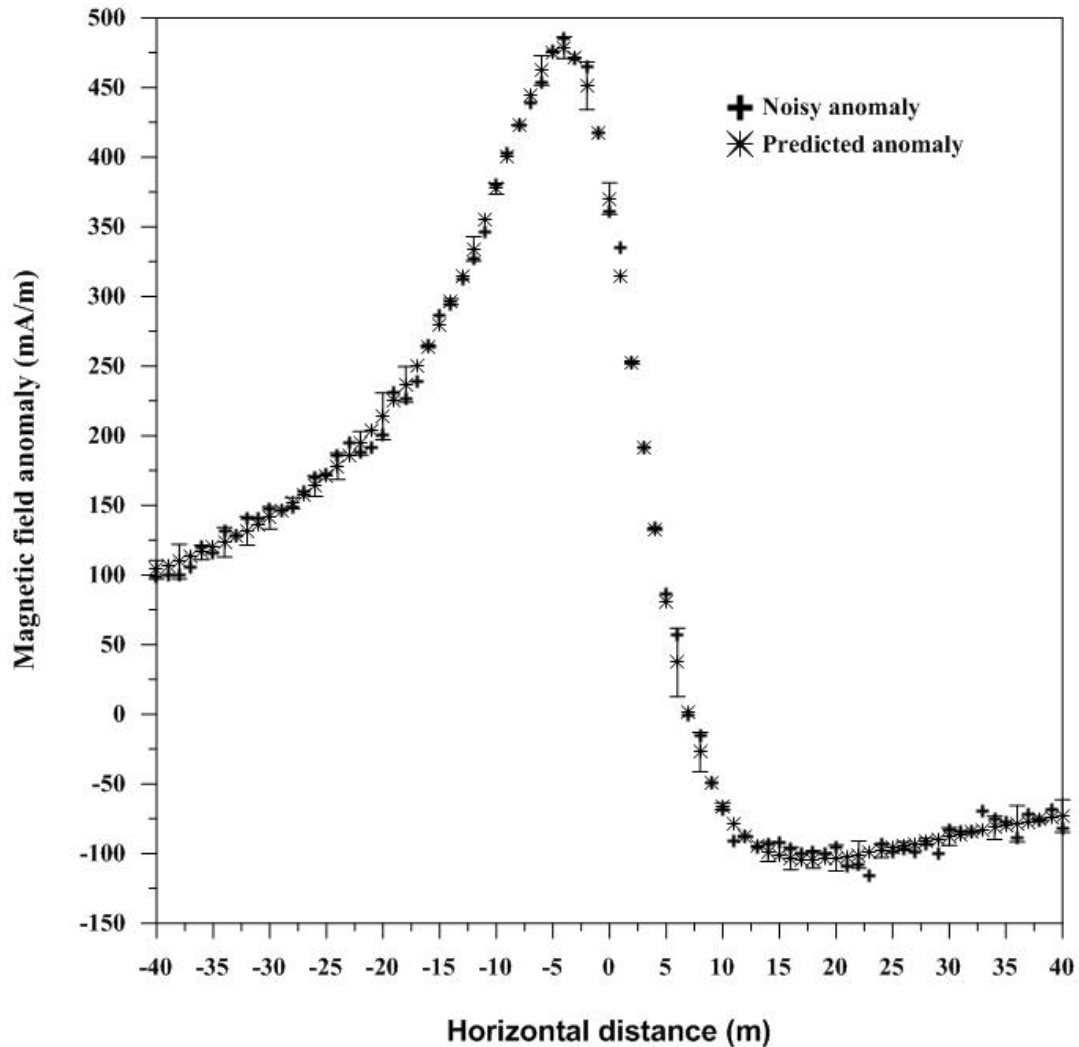
435

Figure 3: Total magnetic anomaly of a buried dipping dike-like a geologic structure with K = 795.78 mA/m, z = 8 m, α = 40º, d= 3, x_o = 0 m, and profile length = 80 m, without and with 10% random Gaussian noise.

440
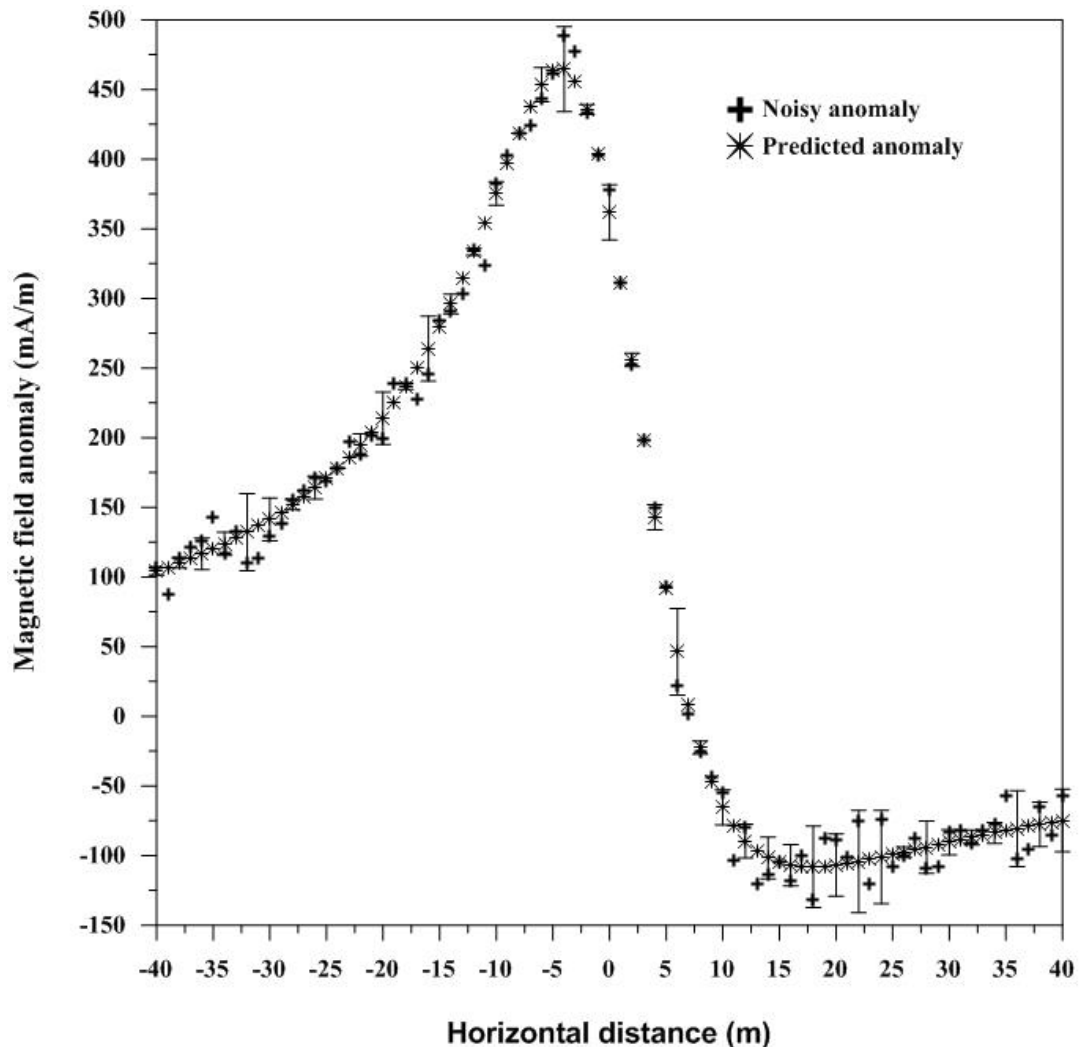
Figure 4: Total magnetic anomaly of a buried dipping dike-like a geologic structure with K = 795.78 mA/m, z = 8 m, α = 40°, d= 3, x_o = 0 m, and profile length = 80 m, without and with 15% random Gaussian noise.

445
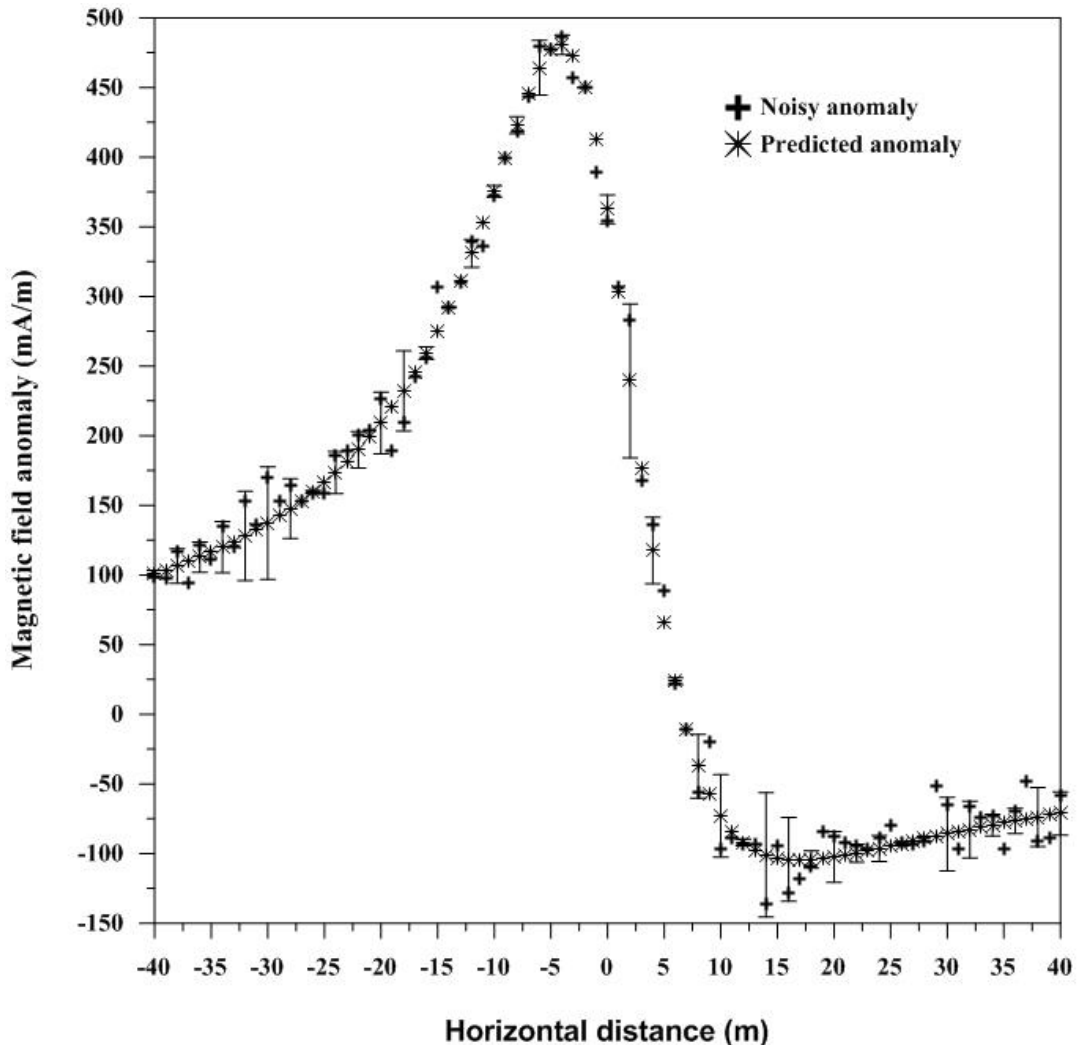
Figure 5: Total magnetic anomaly of a buried dipping dike-like a geologic structure with K = 795.78 mA/m, z = 8 m, α = 40°, d= 3, x_0 = 0 m, and profile length = 80 m, without and with 20% random Gaussian noise.

450

Geoscientific
Instrumentation
Methods and
Data Systems
Discussions
Open Access
EGU

455

460

465

470
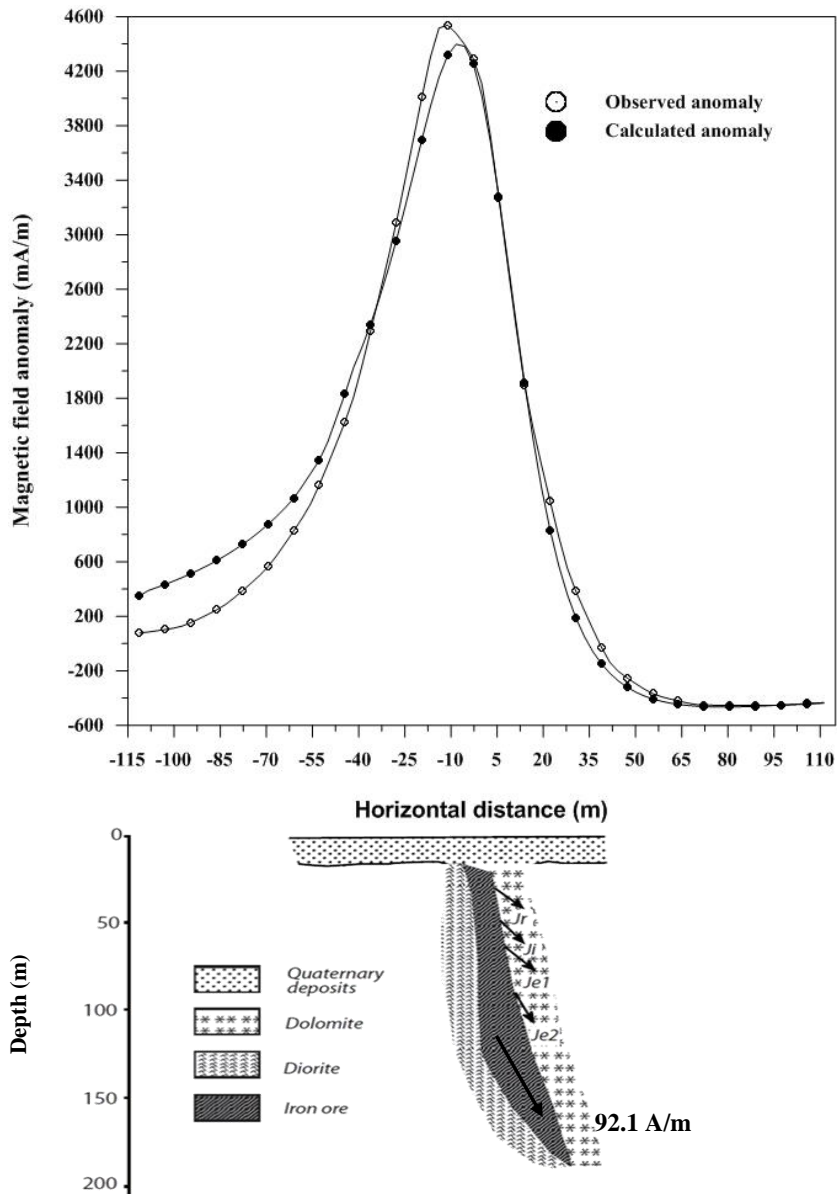
475   **Figure 6: A total magnetic anomaly profile over a magnetite iron deposit, Western Gansu Province, China (open circle) and the estimated magnetic anomaly (black circle) using PSO-algorithm.**
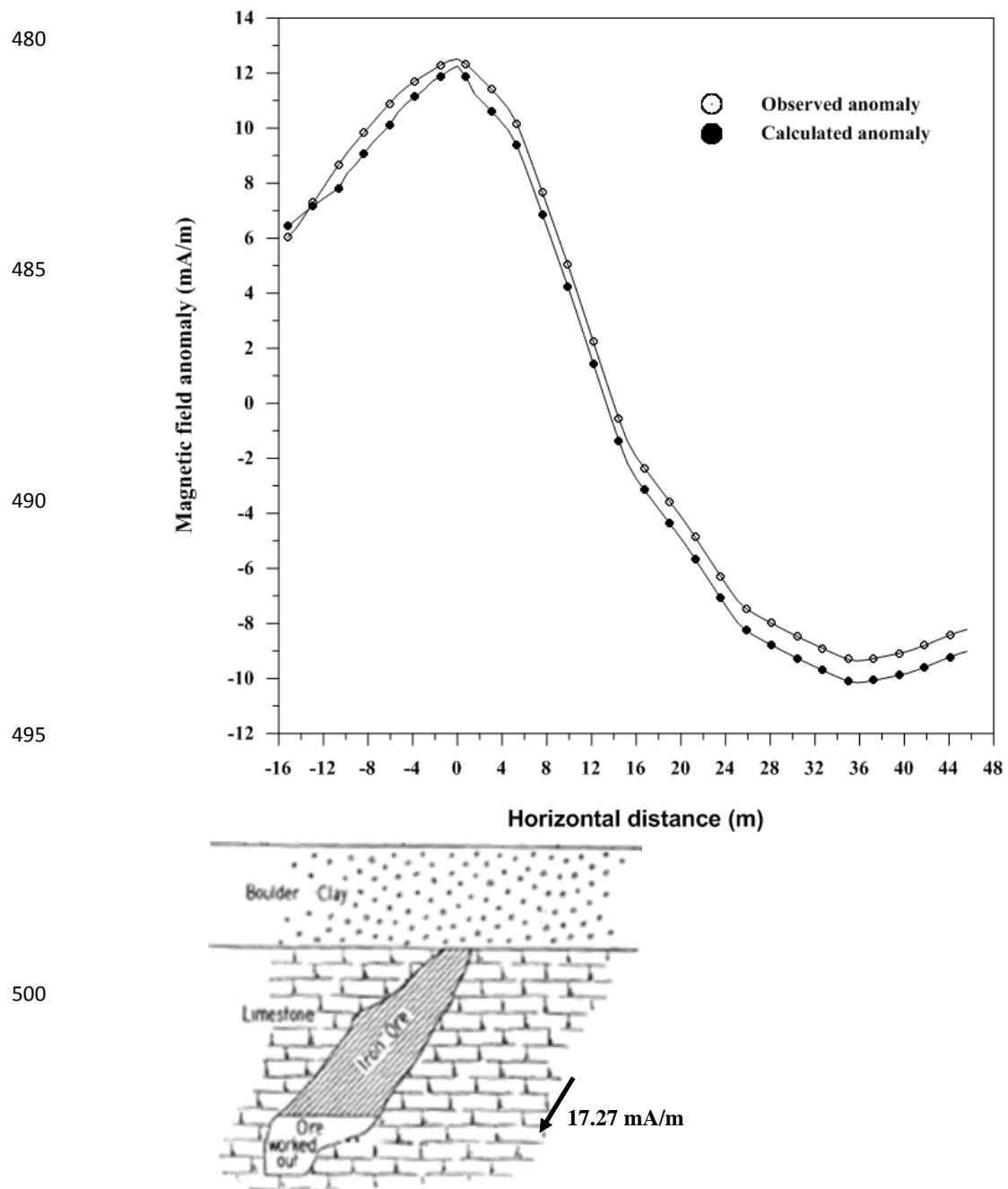
Figure 7: A vertical magnetic anomaly profile over southern Red Hill Farm, Millom, United Kingdom (open circle) and the estimated magnetic anomaly (black circle) using PSO-algorithm.